Surface Tension of Four Alkali Metals to 1000° C.

FERDINAND ROEHLICH, JR., FREDERICK TEPPER, and ROBERT L. RANKIN
MSA Research Corp., Division of Mine Safety Appliances Co., Evans City, Pa. 16033

The surface tension of sodium, potassium, rubidium, and cesium was measured by a maximum-bubble-pressure method at temperatures ranging from the melting point to 1000° C. in a cobalt-tungsten alloy (L-605) chamber. Surface tension–temperature regression lines with standard deviations of 2.5% were derived from the data. The results are compared with those of other investigators and used to determine total surface energy and parachor. A general relationship between surface tension and atomic radius is derived.

RECENT technological advances have yielded increased applications for the alkali metals. An accurate knowledge of the physical properties of these fluids has become vital in many of these applications. One such property, surface tension, is important in wettability and migration effects as well as in atomic bonding studies and in correlation studies with other thermophysical properties. Surface tension values are also utilized in two-phase heat transfer computations.

The surface tension of each of four alkali metals—sodium, potassium, rubidium, and cesium—was determined experimentally between the melting point and 1000° C. These results were used to derive the parachor, the total surface energy, and a relationship between surface tension and atomic radius.

EXPERIMENTAL METHOD

Surface tension values were determined by measuring the maximum pressure required to form and liberate argon-filled bubbles from vertical capillary tubes immersed in the liquid metal. The maximum pressure (P_{max}) required to liberate an inert gas bubble from a tube tip may be expressed as the sum of two component pressures, one of which is related directly to surface tension, as shown below:

$$P_{max} = P_{head} + P_{st} = gh\,(\rho - \rho_o) + \frac{2\gamma}{r} \qquad (1)$$

where P_{head} is the pressure due to the liquid metal head, P_{st} is the force per unit area necessary to create a new surface against the collapsing force of surface tension, h is the head or immersion depth distance, g is acceleration of gravity, ρ is liquid metal density, ρ_o is density of bubble gas (argon), γ is surface tension, and r is the effective radius of bubble formation.

The gas bubbles formed in liquid metals from available capillary tubes are somewhat distorted or nonspherical, because of gravitational and wetting effects. Corrective procedures for nonspherical bubbles have been developed by Schrodinger (*14*), Fesenko (*6*), and Sugden (*16*). The latter two are more precise for tubes of 1- to 2-mm. radius and were used here.

To determine the effective radius of bubble formation, pairs of tubes of decidedly different dimensions—i.e., radii and wall thickness—were incorporated into the apparatus and an accurate micrometer was used to measure tube immersion depths.

MATERIALS

The alkali metals used in these experiments were high purity, research grades. Analyses were performed on each metal used (Table I).

APPARATUS AND PROCEDURE

A sketch of the apparatus is shown in Figure 1. The liquid metal chamber, 11, in which the bubbles are formed consists of a 7-inch-long L-605 alloy container, 3.5-inch outside diameter with a 0.25-inch wall. Three thermocouple wells, 8, are located in the chamber. The apparatus is mounted inside a stainless steel heating block, 3.75-inch inside diameter, 4. Three wire-wound tubular elements, 5, with separate controls on each element, heat the block and chamber to experimental temperatures. Liquid metal is loaded into the chamber from a stainless steel reservoir, 3.

The L-605 alloy capillary tubes, 1, are inserted into the chamber through a 1-inch diameter tube and then centered by manipulation of flange bolts, 12. Their vertical position in the chamber is regulated by means of a micrometer screw feed, 15, and bellows assembly, 9, mounted in the upper end of the 1-inch tube. An electrical circuit, 1, indicates contact of the capillary tube tips with the alkali metal. Argon pressure required to form the bubbles is provided by a motorized bellows assembly, 18, operating at a speed of ~1 r.p.m. The maximum pressure is measured with a dibutyl phthalate–filled differential manometer, 16, read with an optical cathetometer. The tip surface of each bubble tube used is polished to a 0.5-micron alumina finish.

Table I. Typical Analysis of Alkali Metal Purity

Major Impurities	Metal			
	Sodium	Potassium	Rubidium	Cesium
	Impurity Values, Parts Per Million			
Li	20	...	...	...
Na	...	5	30	5
K	100	...	50	<2
Rb	...	...	...	<2
Cs	...	...	500	...
Total	120	50	<0.1%	<10
Alkaline	20	10	10	5
Other	50	40	30	20
Chlorine	14	<5	<5	<5
Oxygen	<10	<10	<20	<20
Nitrogen	...	<2	<2	<2
Carbon	20	20	20	15
Hydrogen	<2	<2	<2	<2

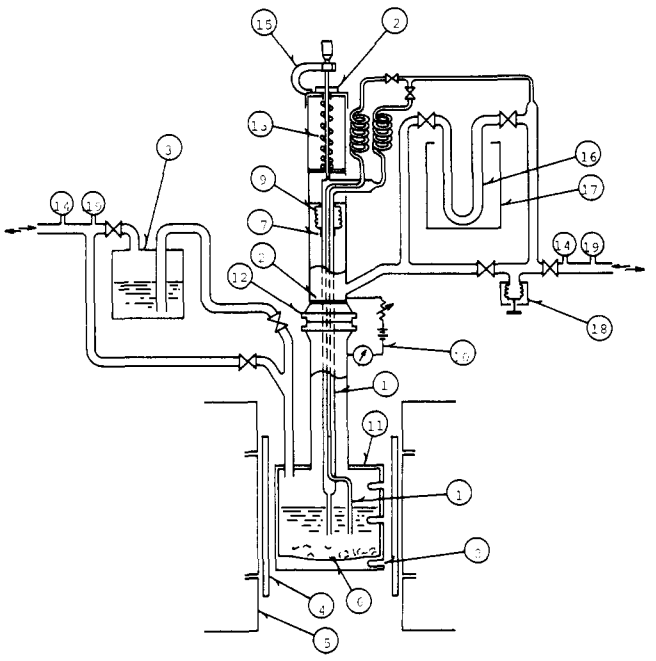

Figure 1. Surface tension apparatus

1. Capillary tubes
2. Guide
3. Alkali metal charging tank
4. Heating block
5. Three-element furnace
6. Zirconium turnings
7. Welded seal
8. Thermocouple wells
9. Bellows
10. Contact-indicating circuit
11. L-605 chamber
12. Flange and insulator
13. Spring
14. Pressure (Bourdon-tube) gage
15. Micrometer
16. Differential manometer
17. Constant temperature bath
18. Motor-driven argon feed
19. Vacuum gage

Its dimensions are measured with a precision microscope to ±0.0002 mm. before it is mounted in the system. The tube tips employed range from 0.744- to 1.600-mm. inside radius and from 0.804- to 1.735-mm. outside radius with wall thicknesses ranging from 0.008 to 0.507 mm.

The apparatus was cleaned and thoroughly degassed to prevent contamination of the liquid metal. A portion of metal was transferred to the chamber by applying argon pressure to the preheated loading tank. The chamber was then heated to ~500° C. for 48 hours to affect gettering by the Zr turnings. When thermal stability was achieved at a particular experimental temperature, the bubble tube tips were immersed a distance of from 1 to 2 cm. (known to approximately 0.005 cm.) beneath the liquid metal surface. Argon pressure was applied alternately to each tube, causing argon bubbles to be formed and liberated at a rate of 5 to 10 per minute. The maximum bubble pressure, as indicated on the differential manometer, was then recorded. Bubble formation rates in the above range were shown experimentally to yield constant maxima.

The surface tension of mercury was measured at room temperature as a preliminary check of the apparatus. A value of 480 dynes per cm. was obtained at 25° C., which is within 1% of the average value of 485 dynes per cm. compiled by White (*20*).

RESULTS AND DISCUSSION

Table II shows surface tension data for each metal in the range of melting point (m.p.) to 1000° C., where various combinations of capillary tubes were used. Experimental points were taken at random temperatures but not in the order listed in the table. From these data, regression line equations were calculated relating surface tension to temperature. The equations are:

$$\gamma Na = 210.12 - 8.105 \times 10^{-2} Z - 8.064 \times 10^{-5} Z^2 + 3.380 \times 10^{-8} Z^3 \quad (2)$$

$$\gamma K = 116.95 - 6.742 \times 10^{-2} Z - 3.836 \times 10^{-5} Z^2 + 3.707 \times 10^{-8} Z^3 \quad (3)$$

$$\gamma Rb = 91.17 - 9.189 \times 10^{-2} Z + 7.228 \times 10^{-5} Z^2 - 3.830 \times 10^{-8} Z^3 \quad (4)$$

$$\gamma Cs = 73.74 - 1.791 \times 10^{-2} Z - 9.610 \times 10^{-5} Z^2 + 6.629 \times 10^{-8} Z^3 \quad (5)$$

where γ is the surface tension in dynes per centimeter, and $Z = (T - T_{m.p.})$ with T in degrees centigrade. The melting point temperatures ($T_{m.p.}$) used were Na 98°, K 64°, Rb 39°, and Cs 28.5° C. The standard deviations of these equations are all less than 3%.

The results for K and Cs were in general agreement with the lower temperature data of other investigations (*4, 5, 12, 18*) with one exception (*17*). However, the Na and Rb surface tension values were higher than reported (*17, 19*) values at corresponding temperatures. The lower results may be attributable to the presence of soluble impurities (*2*). A graphical comparison with other investigators is shown in Figures 2 and 3.

The greatest possible source of error in these experiments and indeed in all experiments involving the maximum-bubble-pressure method lies in the determination of the effective radius of bubble formation. An early analysis (*13*) of this problem showed that the effective radius (r) should change from the external to the internal tube radius as the contact angle falls below 90°. The contact angle of alkali metals on certain metals has been shown to change from about 120° at the melting point to 0° (complete wetting) at some higher temperatures (*2, 9*).

Table II. Surface Tension Data

Sodium		Potassium		Rubidium		Cesium	
Temp., ° C.	Surface tension, dynes/cm.	Temp., ° C.	Surface tension, dynes/cm.	Temp., ° C.	Surface tension, dynes/cm.	Temp., ° C.	Surface tension, dynes/cm.
141	208.0	77	116.9	104	85.4	71	71.6
169	206.0	95	114.0	129	84.8	70	74.4
213	197.6	120	111.9	153	79.5	123	69.9
256	191.6	151	111.0	179	79.8	163	68.5
261	195.4	204	109.0	222	76.5	162	73.1
261	192.7	242	106.9	252	74.2	218	64.1
308	190.7	259	103.8	264	72.7	217	69.5
356	184.7	297	101.1	300	72.8	268	64.9
408	176.0	349	93.6	313	71.6	326	61.5
418	168.0	401	90.5	351	67.7	376	59.5
463	176.5	464	86.5	370	69.7	422	54.5
516	163.9	511	82.8	393	65.3	462	51.3
570	171.2	564	75.6	415	65.3	486	53.3
627	152.8	616	75.7	457	62.0	516	47.6
649	152.7	673	68.8	463	61.4	567	48.0
684	134.8	729	66.0	465	60.7	566	45.9
684	140.0	783	61.9	509	61.3	624	45.2
729	132.6	846	59.4	513	57.6	674	43.6
730	135.2	897	53.6	515	60.5	742	34.8
784	129.2	947	56.4	564	58.2	793	34.2
782	124.0	993	49.6	613	57.9	851	29.6
793	122.4			613	55.9	858	29.0
842	115.1			619	52.8	867	27.9
890	116.0			649	50.7	883	30.6
893	111.0			671	51.8	962	25.7
992	99.5			724	49.9	986	29.1
				738	48.7	1011	26.6
				779	48.0		
				841	45.4		
				906	40.5		
				906	39.8		
				963	40.4		
				1006	33.5		

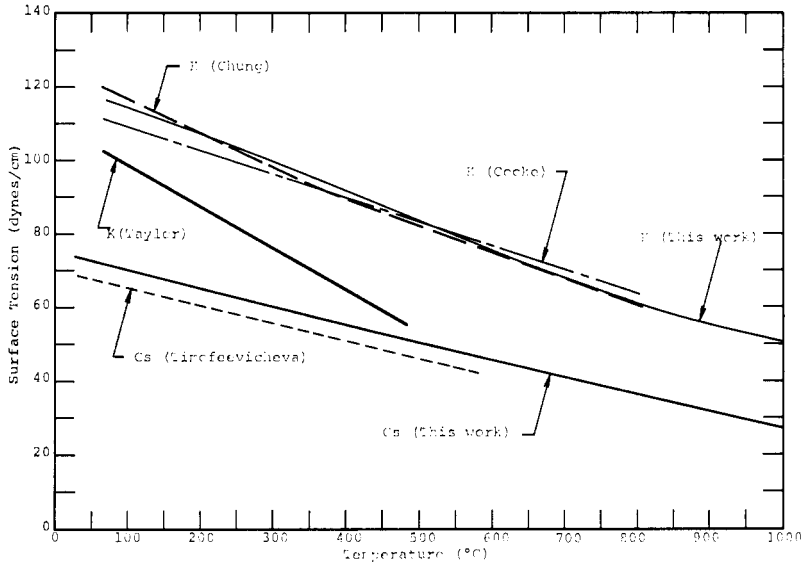

Figure 2. Results for potassium and cesium

To determine the radius of bubble formation for each alkali metal throughout the entire temperature range covered, the following method was employed:

Radial dimensions specified in choosing bubble-formation capillary tubes were such that the ratio of radius to capillary constant expected would be near unity (1.0) for either internal or external radius. This means that the required corrections for bubble sphericity (*16*) were minimal.

One tube of the pair chosen for application to a given alkali metal had a very thin wall (~0.1 mm.), while the other tube was thick-walled (~0.7 mm.). Either the external or the internal radii of each tube pair chosen were identical, however. Each pair of tubes were mounted in the apparatus in such a manner that their tips remained in a common plane when immersed in the liquid metal.

The tips were immersed below the surface of the liquid metal. Argon pressure was applied to only one tube and the maximum bubble pressure noted. Argon was then applied to the other tube and maximum bubble pressure recorded. Hence if the two maxima were similar, the bubble was assumed to form on the radius which was common to both tubes. If the pressure maxima differed in magnitude, it was assumed that the dissimilar radii were the ones on which the bubbles formed.

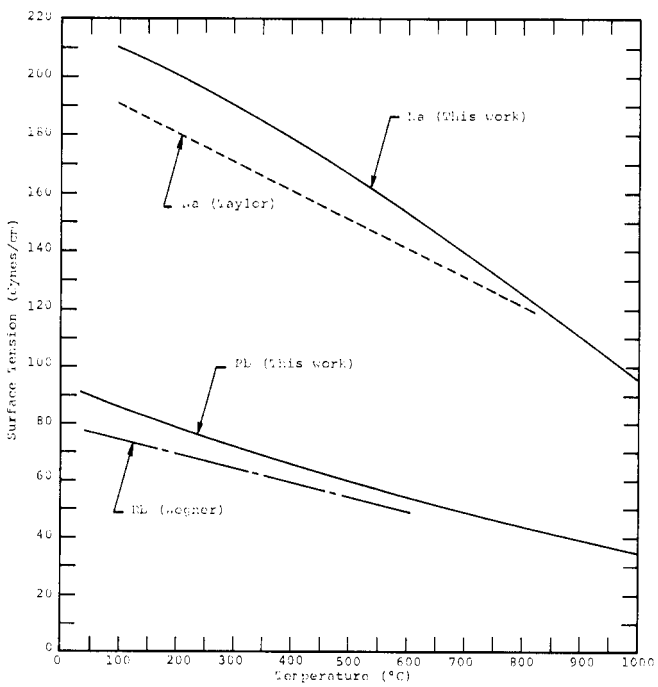

Figure 3. Results for sodium and rubidium

In some of the experiments a thick-walled tube was combined with a thin-walled one, while in others two thin-walled tubes of significantly different radii were employed. In each case the radius of the bubble was corrected by the iterative method developed by Sugden (*16*).

A quantity of some theoretical and practical value in studies of surface properties is the parachor (P), which relates surface tension to density and molecular weight. It is defined as:

$$P = \frac{A\gamma^{1/4}}{\rho' - \rho''} \approx A\gamma^{1/4}/\rho \tag{6}$$

where A = molecular weight, ρ' = density of the liquid, and ρ'' = density of the saturated vapor.

Although the parachor is temperature-independent for many liquids, it increases with increase in temperature for the alkali metals. The parachor was evaluated at three temperatures (melting point, 500° C., and 1000° C.) for each metal. As shown in Table III, the variation of the parachor value with temperature is greatest for cesium and smallest for sodium.

Another quantity of particular importance is the total surface energy. Surface tension, when stated in units of ergs per square centimeter, may be considered a Gibbs free energy, since it can (in principle at least) be transformed into work at constant temperature and pressure. By definition

$$G = H - TS \tag{7}$$

and

$$S = -\left(\frac{\delta G}{\delta T}\right)_p \tag{8}$$

Substituting γ for G we have

$$H = \gamma_T - T\left(\frac{\delta \gamma}{\delta T}\right)_p \tag{9}$$

where H is the surface enthalpy or total surface energy and the quantity

$$-T\left(\frac{\delta \gamma}{\delta T}\right)_p$$

Table III. Parachor and Total Surface Energy

Metal	Temp., °C.	Surface Tension, Dynes/Cm.	Parachor	Total Surface Energy, Ergs/Sq. Cm.
Na	98.0	210.1	94.8	246.7
	500.0	166.7	98.2	242.9
	1000.0	96.2	99.9	221.7
K	64.0	116.95	157.4	141.9
	500.0	83.3	162.6	140.4
	1000.0	50.6	170.7	144.7
Rb	39.0	91.2	179.9	105.8
	500.0	60.4	182.8	96.6
	1000.0	35.6	195.7	95.2
Cs	28.5	73.7	211.2	90.0
	500.0	51.2	224.1	92.9
	1000.0	26.4	235.3	95.1

Table IV. Surface Tension Derived from Atomic Radius Correlation

Metal	Temp., °C.	Surface Tension, Dynes/Cm. Calcd.	Regression line	%
Cs	500	49.5	51.2	−3.4
	1000	23.9	26.4	−10.5
Rb	500	63.7	60.4	+5.2
	1000	33.9	35.6	−5.0
K	500	87.7	83.3	+4.8
	1000	54.2	50.6	+6.6
Na	500	171.4	166.7	+2.7
	1000	123.2	96.2	+21.9
Hg (*15*)	360	429	392	+9.4
Sn (*11*)	400	599	594	+0.8
	800	524	520	+0.8
U (*3*)	1575	1416	1488	−4.8
Bi (*10*)	400	373	374	−0.3
	600	341	343	−0.5

is the latent heat of the surface (*1*). The value of H at a given temperature is a measure of the decrease in enthalpy associated with the destruction of 1 sq. cm. of liquid surface. It is a factor in the determination of the area of a finely divided crystalline solid (*8*) and may be useful in heat transfer problems involving vapor nucleation. Total surface energies were evaluated at the melting point, at 500° C., and at 1000° C. (Table III). Straight-line (constant-slope) representations of the data were used to evaluate the derivative.

A general analysis of the surface properties of metals indicates that surface tension may be a function of the atomic radius. The following empirical relationship was derived based on the present results:

$$\gamma_T = \gamma_{m.p.} - \left[\frac{T - T_{m.p.}}{3\sigma^2} \right] \quad (10)$$

where σ is the atomic radius in angstroms and subscript m.p. refers to values of γ and T at the melting point.

Predicted values of γ at 500° and 1000° C. were calculated by this equation (Table IV). Melting point values were obtained from the experimental data regression lines. The same expression was applied also to mercury, tin, uranium, and bismuth (Table IV). The surface tension data were obtained from the references indicated. Atomic radii values were obtained from the "Handbook of Chemistry and Physics" (*7*). This correlation should be of some value in predicting surface tension values at higher temperatures where direct measurements become difficult.

LITERATURE CITED

(1) Adam, N.K., "The Physics and Chemistry of Surfaces," Oxford University Press, London, 1941.
(2) Addison, C.C., *J. Chem. Soc. (London)* **1954**, 2861; **1955**, 3047.
(3) Cahill, J.A., Kirshenbaum, A.D., *J. Nucl. Chem.* **27**, 73–6 (1965).
(4) Chung, J.W., U.S. Atomic Energy Comm. Rept. **CU-2660-16** (March 1965).
(5) Cooke, J.W., Oak Ridge National Laboratories, Proceedings of 1963 High Temperature Liquid Metals Heat Transfer Technical Meeting, ORNL-3605, UC-33, TID-4500 (34th), Vol. 1 (November 1964).
(6) Fesenko, V.V., *Russian J. Phys. Chem.* **35**, No. 4, 345 (April 1961).
(7) "Handbook of Chemistry and Physics," Chemical Rubber Publishing Co., Cleveland, Ohio, 41st Ed., 1962–3.
(8) Harkins, W.D., Jura, G., *J. Am. Chem. Soc.* **66**, 1362 (1944).
(9) Hoffman, J.W., Keyes, J.J., Jr., Oak Ridge National Laboratories, AEC Rept. **ORNL-TM-915**, 105–8 (October 1964).
(10) Matuzama, U., *Sci. Repts. Tohoku Imp. Univ.*, **16**, 69 (1927).
(11) Pelzel, E., *Berg-. Hüttenmänni. Monatsh. Montan. Hochschule Leoben* **93**, 247 (1948); **94**, 10 (1949).
(12) Poindexter, F.E., Kernaghan, M., *Phys. Rev.* **33**, 837 (1929).
(13) Porter, A.W., *Phil. Mag. Sci.* **9**, No. 61, 7 (June 1930).
(14) Schrodinger, E., *Ann. Physik* **46**, 137 (1914).
(15) Smithells, C.J., "Metals Reference Book," p. 416, London Publishing, London, 1949.
(16) Sugden, S., *J. Chem. Soc. (London)* **121**, 858 (1922).
(17) Taylor, J.W., *J. Inst. Metals* **83**, 143–52 (1955).
(18) Timofeevicheva, O.A., *Dokl. Akad. Nauk, SSR* **143**, 618 (1962).
(19) Wegner, H., *Z. Physik* **143**, No. 5, 548 (1959).
(20) White, D.W.G., *Am Soc. Metals Trans. Quart.* **55**, 767 (1962).

RECEIVED for review November 16, 1966. Resubmitted March 20, 1968. Accepted May 24, 1968. Part of a program sponsored by the U.S. Air Force, Research and Technology Division, Wright-Patterson Air Force Base.